Magnetic structure of $^{154}SmMn_2Ge_2$ as a function of temperature and pressure

G. J. Tomka*
Department of Physics and Astronomy, University of St. Andrews, St. Andrews, Fife KY16 9SS, United Kingdom

C. Ritter
Institut Laue Langevin, Avenue des Martyrs, BP 156, F-38 042, Grenoble Cedex 9, France

P. C. Riedi
Department of Physics and Astronomy, University of St. Andrews, St. Andrews, Fife KY16 9SS, United Kingdom

Cz. Kapusta and W. Kocemba
Department of Solid State Physics, Faculty of Physics and Nuclear Techniques, University of Mining and Metallurgy, 30-059 Cracow, Poland

(Received 10 March 1998)

Neutron scattering, ac susceptibility, and NMR measurements have been made on isotopically enriched $^{154}SmMn_2Ge_2$. All the magnetic states are characterized from much clearer neutron-diffraction spectra than in previous works, in which natural abundance Sm was used. A temperature versus pressure magnetic phase diagram is proposed, consisting of six distinct magnetic states, including previously undetected incommensurate cone structures at low temperatures and pressures. The noncollinear magnetic structures of these magnetic phases are such that a larger antiferromagnetic component appears within (001) planes in the ferromagnetic states than in the antiferromagnetic states. This observation provides an explanation for the anisotropic changes in the lattice constant and the anomalous magnetoresistance of $SmMn_2Ge_2$. Previously unexplained susceptibility and NMR measurements are interpreted in terms of changes to the cone structure. Changes in the Mn-Mn spacing and magnetic coupling are consistent with previous observations on related systems.
[S0163-1829(98)05033-4]

I. INTRODUCTION

The ternary compound $SmMn_2Ge_2$ is the most unusual member of the RT_2X_2 family of naturally layered materials (R is rare earth, T is transition metal, X is Si or Ge). These materials crystallize in the body-centered-tetragonal $ThCr_2Si_2$ (space group $I/4mmm$) and consist of atomic layers stacked in the sequence R-X-T_2-X-, with R, T, and X atoms occupying the $2a$, $4d$, and $4c$ sites respectively.[1] The magnetic behavior of $SmMn_2Ge_2$ was explored by Fujii *et al.* using dc magnetization measurements,[2] and revealed a sequence of magnetic phase transitions. There is a transition from a paramagnetic to a c axis ferromagnetic state (FM1) at a temperature $T_{t1} \approx 350$ K. This gives way to an antiferromagnetic state (AFM1) below $T_{t2} \approx 150$ K and there is a transition to an ab-plane ferromagnetic ground state (FM2) at $T_{t3} \approx 100$ K. Fujii *et al.* postulated that the Mn-Mn coupling within layers remained ferromagnetic (FM) in all three magnetic phases, and suggested that the transition to the low-temperature FM phase, FM2, was driven by a magnetic ordering of the Sm sublattice. This mechanism, however, was found to be inconsistent with the small entropy change ($< R/10 \ln 2$), associated with the transition.[3] As well as exhibiting reentrant ferromagnetism, $SmMn_2Ge_2$ has other unusual properties. It was found from an x-ray study by Gyorgy *et al.*,[3] and by neutron scattering,[4] that the change in the lattice constant through both transitions was anisotropic, with a larger change in the a direction than in the c direction. This is unexpected if the in-plane magnetic coupling remains unchanged through the transition.

The compound is of further interest because of the giant magnetoresistance (GMR) present in the antiferromagnetic phase, AFM1. The magnitude of the GMR was about 8% for a current perpendicular to the c axis with a field in the c direction. The GMR, however, was found to be of the opposite sign to that found in most artificial multilayers, with resistance increasing, rather than decreasing, in a magnetic field.[5]

Despite the interest in the magnetic properties of $SmMn_2Ge_2$, until recently[4] the material had not been studied by neutron diffraction because of the very large absorption cross section of ^{149}Sm, which is $\sim 14\%$ abundant in natural Sm. In the recent neutron-scattering experiment,[4] measurements were performed on finely powdered natural $SmMn_2Ge_2$, diluted with Al powder in a ratio of 1:10. Despite the large background absorption, it was possible to derive magnetic structures from the spectra. It was found that the simple model of collinear structures proposed by Fujii *et al.* was inconsistent with the data. Rather, the magnetic structure of each phase had to consist of a noncollinear arrangement of moments. In this paper an analysis of the much better data, provided by measurements on a sample containing isotopically enriched Sm, revealed the presence of satellites to the (101) line in the AFM1 and FM2 states, indicating the existence of a much more complicated cone structure.

It has been found that the application of pressure has the effect of stabilizing the AFM state.[3,6,7] The behavior of T_{t3} as a function of pressure was measured by Lord *et al.* using ^{55}Mn NMR. The value of dT_{t3}/dP at low pressure was found to be about -16 K/kbar, with its magnitude decreasing at higher pressure. Recently, the related system $SmMn_2(Ge_{1-x}Si_x)_2$ has received attention,[8,9] since the par-

tial substitution of Ge by Si provides an alternative method of altering the effective interatomic spacing. Saha and Ali[8] have argued that, for changes in the nonmagnetic constituent, the main effect on the magnetic properties is likely to arise from changes in the lattice constant. Indeed, the x-T phase diagram of Saha and Ali[8] is remarkably similar to the T-P phase diagram of Lord *et al.*,[6] with an increase in x of 0.1, equivalent to an increase in pressure of about 6.6 kbar.

However, this ''chemical pressure'' by substitution may not have the same effect on the magnetic properties of the system as that obtained by the application of hydrostatic pressure. For example, we have found[10] that applied pressure on $NdMn_2Ge_2$ does not induce the low-temperature c-axis ordering found in $NdMn_2Si_2$. Our ^{55}Mn NMR measurements of $NdMn_2Ge_2$ under pressure have shown that there is remarkably little change in the low-temperature magnetic structure with applied pressure, and neutron-scattering measurements suggest that applied pressure may actually increase the stability of the a-b plane FM.[10]

NMR measurements[6] have shown that the ^{55}Mn frequency of $SmMn_2Ge_2$ increases with increasing temperature in the range 3–75 K, despite the decrease in magnetization by some 16%. Lord *et al.*[6] suggested that both the decrease in magnetization and increase in the ^{55}Mn frequency was attributable to a decrease in the Sm moment, since the transferred hyperfine field from the Sm is positive with respect to the Mn moment direction, whereas the contact interaction with the Mn spin of the parent atom induces a predominantly negative hyperfine field at the Mn nucleus. A direct observation of changes in the ^{147}Sm and ^{149}Sm NMR was not possible above 19 K because of the rapid increase of the transverse relaxation rate with temperature, so the authors could not conclusively show that the Sm moment had no influence on the AFM-FM transition at T_{t3}.

Lord *et al.* also pointed out that the observed changes in the width of the ^{55}Mn NMR line may reflect changes in the structure of the Mn sublattice. They suggested that the differences in the local anisotropy of the Sm and Mn sublattices and the competition between interplanar Mn-Mn interactions, and intraplanar Mn-Sm/Mn-Mn interactions, lead to noncollinearity between Sm and Mn moments. A remarkable feature of the Sm NMR is that the resonance frequency at a given temperature is independent of pressure, although the Mn NMR frequency decreases with pressure.

In this paper we present neutron-scattering data, which are much clearer than it was possible to obtain in earlier works,[4] using natural abundance Sm. We present information on the magnetic and structural properties of $SmMn_2Ge_2$ as a function of temperature and pressure, and discuss the results in relation to the NMR, magnetization, and transport properties of the system. Changes in the magnetic structure provide an explanation for the anisotropic changes in the lattice constant and the anomalous magnetoresistance of $SmMn_2Ge_2$. Previously unexplained susceptibility and NMR measurements are interpreted in terms of changes to the cone structure, and changes in the Mn-Mn spacing and magnetic coupling are shown to be consistent with previous observations on related systems. A temperature versus pressure magnetic phase diagram, consisting of six distinct magnetic states, is presented, including previously undetected incommensurate cone structures at low temperatures and pressures.

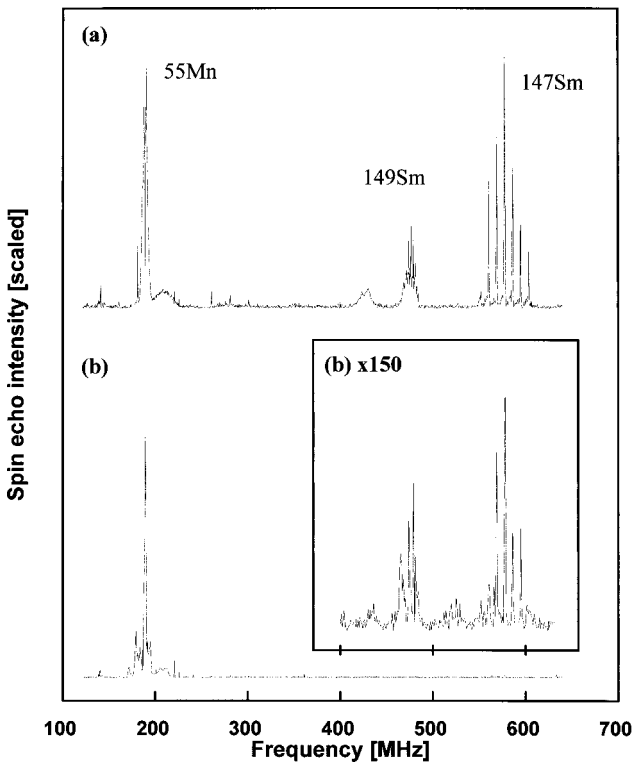

FIG. 1. Comparison of NMR spectrum of natural abundance $SmMn_2Ge_2$ used previously (Ref. 10) and the ^{154}Sm enriched sample. The inset shows that, by removing attenuators on the receiver, it is still possible to detect ^{147}Sm and ^{149}Sm nuclei.

II. EXPERIMENTAL

Measurements were made on a finely powdered sample of $SmMn_2Ge_2$ prepared from isotopically enriched ^{154}Sm. The sample was prepared from high-purity constituent elements. A stoichiometric mixture was first melted in an argon atmosphere using an induction furnace. The resulting pellet was repeatedly melted in an argon arc furnace, wrapped in Ta foil, and annealed for 5 days in an argon atmosphere at 800 °C. The final sample was checked by powder x-ray diffraction and confirmed to be single phase $SmMn_2Ge_2$.

Figure 1 shows a comparison of the NMR spectrum of the natural abundance sample used in the earlier neutron-scattering experiment[4] and the ^{154}Sm enriched sample. The ^{55}Mn spectra have been approximately scaled to the same peak intensity. The spectra indicate that the sample contains less than 0.2% of the highly absorbing ^{149}Sm isotope. This is consistent with the manufacturer's isotopic analysis that indicated the presence of 0.17 ± 0.02 at. % ^{149}Sm.

NMR measurements were made using a fully automated, phase-coherent swept frequency spectrometer with the sample in an untuned sample coil.[11] All the spectra in Fig. 1 were produced under identical conditions of pulse spacing, length, and power conditions, optimized for the ^{149}Sm spectra. These conditions are overpowered for the ^{55}Mn nuclei resulting in an apparent structure to the line. The dependence of the ^{55}Mn resonance line shape in $SmMn_2Ge_2$ on the power is discussed in detail elsewhere.[6]

Susceptibility measurements were made using an ac compensated coil system, with temperatures swept at a rate of less than 0.5 K min^{-1}. The high-pressure NMR and ac sus-

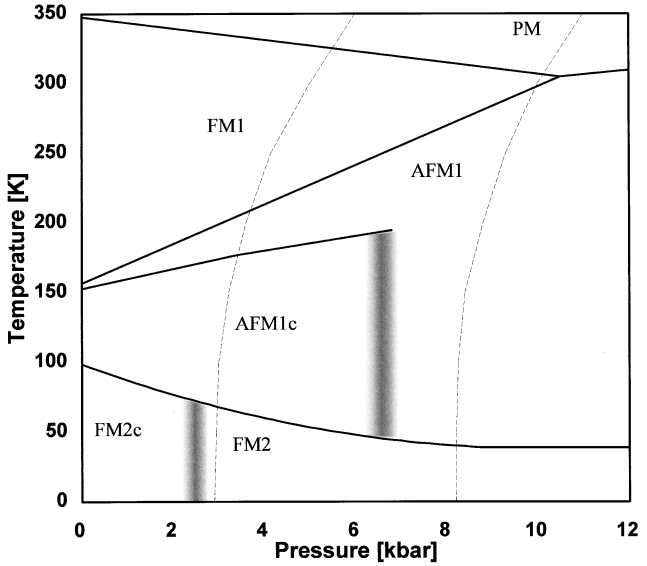

FIG. 2. Proposed magnetic T-P phase diagram for $SmMn_2Ge_2$: PM-Paramagnetic. FM1-FM along $\langle 001 \rangle$, AFM component in (001) planes. AFM1-AFM lying along $\langle 001 \rangle$, net FM component within each (001) plane, and additional AFM coupling between neighbors within (001) planes. AFM1c-as AFM1, with cone, propagation vector in the $\langle 001 \rangle$ direction. FM2-FM component in the (001) plane, AFM coupling within (001) planes, and additional AFM coupling along $\langle 001 \rangle$. FM2c-as FM2 with cone, propagation vector along $\langle 001 \rangle$. The grey bars indicate speculative values for the pressure required to cause the cone structure to collapse. The dotted lines are indicative of changes of pressure in the clamped cell.

ceptibility experiments were carried out in a Be-Cu pressure cell. The pressure was applied to the liquid immersed sample at room temperature and locked into the cell. The cell could then be removed from the press and cooled to low temperature. The pressure was measured using the resistance of a calibrated semiconductor transducer. The maximum pressure obtained at 13 K was 8.8 kbar.

Neutron-diffraction measurements were performed on D1B at the ILL, with $\lambda = 2.52$ Å. Measurements were made at atmospheric pressure in a standard tube sample holder, and also under pressure as a function of temperature, with pressures of 5 and 10 kbar locked in to a zero matrix, flourinert filled pressure cell. Measurements were made under similar conditions of the lattice constants of NaCl as a function of temperature. This allowed an estimate of the pressure in the cell as a function of temperature to be made. Magnetic structures and moments of the Mn and Sm sublattices were calculated using the Rietveld refinement program FULLPROF. The spectra were refined under the assumption that the Sm moment couples FM to the FM component of the Mn sublattice.

III. RESULTS

The changes in the magnetic structure of $SmMn_2Ge_2$ with temperature and pressure are complicated. The proposed temperature versus pressure magnetic phase diagram, Fig. 2, summarizing our results is shown as a guide, and the principle magnetic structures are shown in Fig. 3.

A. Susceptibility and NMR measurements

Part of the temperature dependence of the ac susceptibility of $SmMn_2Ge_2$ is shown in Fig. 4. The zero pressure data are similar to those obtained in previous experiments,[3,4,8] with transitions $T_{t3} = 99$ K and $T_{t3} = 157$ K. The measurements were performed at a high sensitivity to show a small but clear anomaly at $T_{cc} = 153$ K. The figure also shows the effect of the application of pressure. We have found that at 8.8 kbar the T_{t3} transition has dropped to 39 K, due to the increase in stability of AFM1. No other transitions were observed in the temperature range 10–270 K. The transition T_{cc} has been ascribed to a spin reorientation,[8] though this explanation of the transition is inconsistent with the neutron-scattering measurements.[4] The measurements of Saha and Ali[8] on $SmMn_2(Ge_{1-x}Si_x)_2$ have shown that the transition temperature T_{cc} is nearly independent of Si substitution. They are able to observe this transition up to $x = 0.15$, equivalent to a real pressure of about 10 kbar, however we were not able to find this transition with ac susceptibility at 8.8 kbar in $SmMn_2Ge_2$.

Zero-field NMR measurements also reveal the increasing stability of AFM1 at high pressure as shown in Fig. 5. The ^{55}Mn NMR signal was not observable in the AFM state due to the disappearance of FM domain walls, which enhance the observed signal. Zero-field NMR in the FM material also provided a means of monitoring the local field at the ^{147}Sm and ^{149}Sm nuclei, and could therefore give an indication as to whether the FM ordering at T_{t3} is being driven by an ordering of the Sm sublattice. Unfortunately, above 19 K, the transverse relaxation time became too short for a Sm signal to be observed. This prohibited a reliable extrapolation to find the temperature at which the Sm moment collapses. Indirect evidence of the behavior of the Sm moment below T_{t3} is obtained from changes in the ^{55}Mn NMR frequency and linewidth. This is discussed below in relation to the information obtained from neutron-scattering measurements.

B. Neutron scattering at zero pressure

Neutron-scattering data for measurements made at ambient pressure are presented in the neutron thermogram, Fig. 6. The changes in the neutron-diffraction pattern with temperature reflect the changes in the magnetic structure. For example, the satellite lines to the (101) line at 38.7° indicate the formation of an incommensurate cone structure, and the appearance of a line at 68.5° between the nuclear peaks is indicative of the evolution of AFM between T_{t2} and T_{t3}. The best magnetic structures of $SmMn_2Ge_2$, as derived from Rietveldt refinements, are detailed below.

Below 100 K there is a net FM component ($\sim 2\mu_B$) in the a-b plane, with an AFM component ($\sim 2.2\mu_B$) in the c direction, such that neighboring Mn moments within the a-b plane are spin canted. Neighbors in the c direction are also AFM coupled. A cone with a propagation vector in the c direction is observed. A small magnetic moment is found for the Sm sublattice, oriented parallel to the ferromagnetic component of the Mn sublattice. Figure 3(a) shows this complicated structure, which we call FM2c. Changes with temperature in the cone angle (open squares) and in the propagation vector of the cone (filled squares) are shown in Fig. 7. Confidence limits on the refinement are better than 0.004 on the

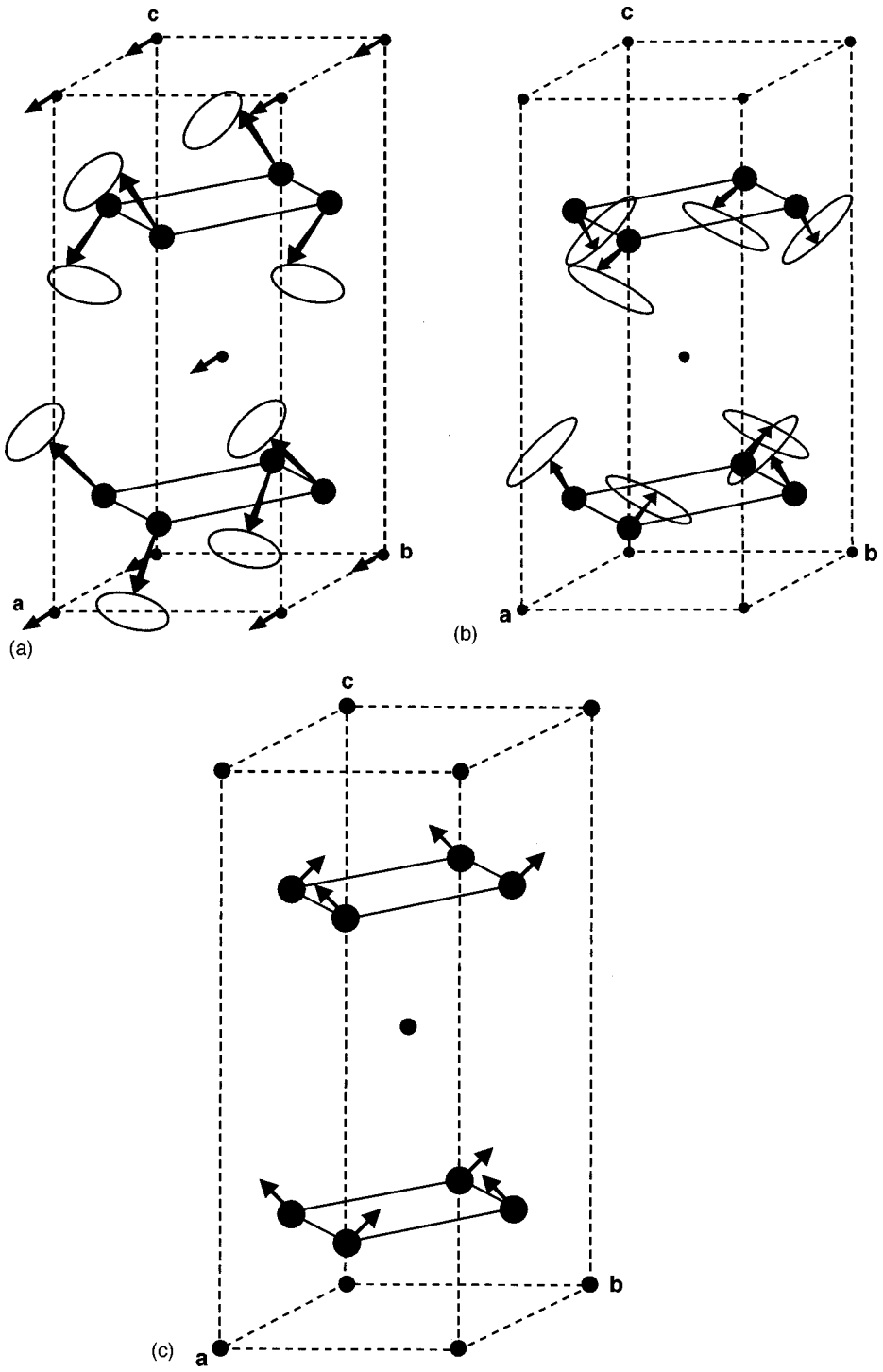

FIG. 3. The principal magnetic phases of $SmMn_2Ge_2$: (a) FM2c, (b) AFM1, and (c) FM1.

propagation vector and better than 5° on the cone angle. The Mn moment is $3.0\mu_B$ at 1.5 K and drops to $2.8\mu_B$ at 98 K. The Sm moment varies between $0.65\mu_B$ to $0.3\mu_B$ in the same regime, as shown in Fig. 8. In zero pressure, confidence limits on the refinement of the moments are better than $0.06\mu_B$ for the Mn sublattice and better than $0.1\mu_B$ for the Sm sublattice.

Between 100 and 154 K the Mn moments have a net AFM structure. Within *a*-*b* planes, moments of nearest neighbors are coupled AFM, with an AFM component of $1.6\mu_B$ in the plane, but with a FM component of $2\mu_B$ along the *c* axis. Neighbors in the *c* direction are coupled antiparallel [Fig. 3(b)]. A cone with a propagation vector parallel to the *c* axis is observed, with a maximum cone angle at around 128 K, as shown by open squares in Fig. 7. The total Mn moment in this regime is around $2.6\mu_B$. We call this structure AFM1c.

Above 154 K the structure again has a FM component ($\sim 1.7\mu_B$). Unlike in the low-temperature FM state, however, the FM component is in the *c* direction. An AFM component ($\sim 1.9\mu_B$) exists within the *a*-*b* plane, with an AFM coupling of this component both between nearest neighbors

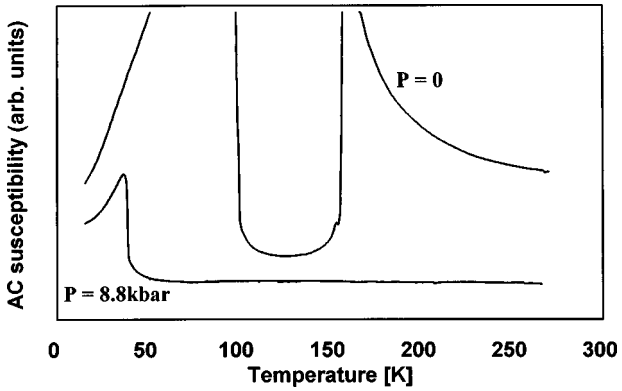

FIG. 4. Part of the temperature dependence of the ac susceptibility of $SmMn_2Ge_2$, showing the presence of an anomaly at 153 K at zero pressure. No such anomaly is observed at 8.8 kbar.

and neighbors in the c direction, as illustrated in Fig. 3(c). The total Mn moment in this regime is around $2.5\mu_B$. We call this structure FM1. The refinement indicates that there may be a Sm moment in this regime of around $0.6\mu_B$, though as for the intermediate phase (100–154 K), a good refinement could also be obtained with no moment on the Sm sublattice.

Our neutron-scattering measurements have provided information on the thermal expansion of the system to a higher accuracy than earlier x-ray scattering data.[3] The data are shown for thermal expansion in the a direction, Fig. 9(a), and in the c direction, Fig. 9(b). On cooling through T_{t2}, the a axis was found to contract by some $0.20\pm.01\%$ and was found to expand again by the same amount at T_{t3}, but the jump in the c-axis direction was an increase of $0.055\pm.01\%$ in the AFM state.

C. Neutron-scattering measurements under pressure

Measurements were made in the zero matrix (i.e., low background), flourinert filled pressure cell with 5 kbar locked in at room temperature. The refinement of the data from the measurements made in the pressure cell allowed for the

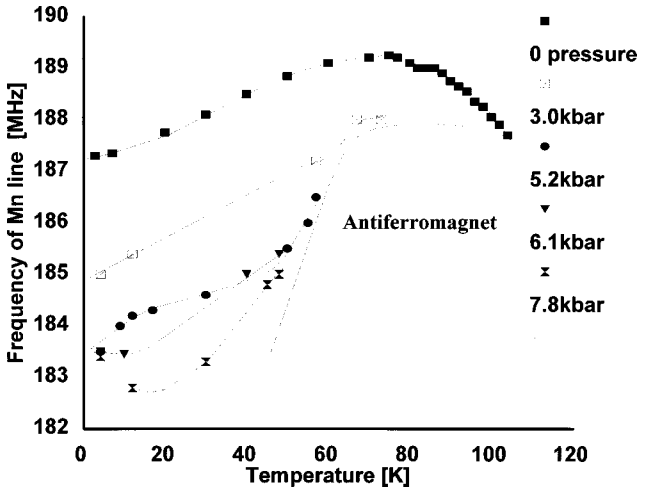

FIG. 5. Variation of the ^{55}Mn NMR frequency as a function of temperature in the FM2 phase for a series of pressures. No signal is observed in the antiferromagnetic phase because of the absence of domain-wall enhancement effects. Lines are guides to the eye.

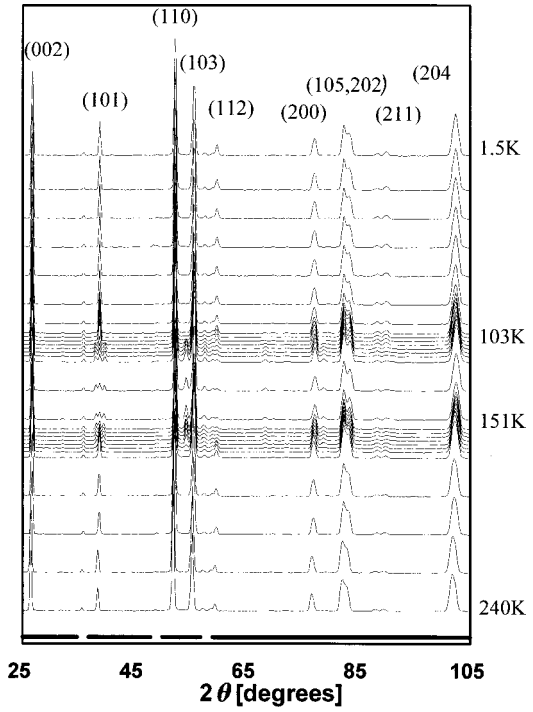

FIG. 6. Neutron thermogram of $SmMn_2Ge_2$. The principal reflections are indexed and temperatures are indicated for some spectra. The regions excluded from the refinement due to background contributions from the cryostat are indicated by the gaps in the bold line at the base of the thermogram.

variation of a preferred orientation of crystallographic directions as a function of temperature. It was found that this parameter followed changes in the sample volume. The results of the neutron-scattering measurements are shown in Fig. 10 and are detailed below. The larger background seen in this figure, compared with Fig. 6, comes from the pressure cell. A reliable refinement of the Sm moment was not possible when the sample was in the pressure cell. This was due to the larger background and the association between the Sm moment and the preferred orientation parameter in the refinement process.

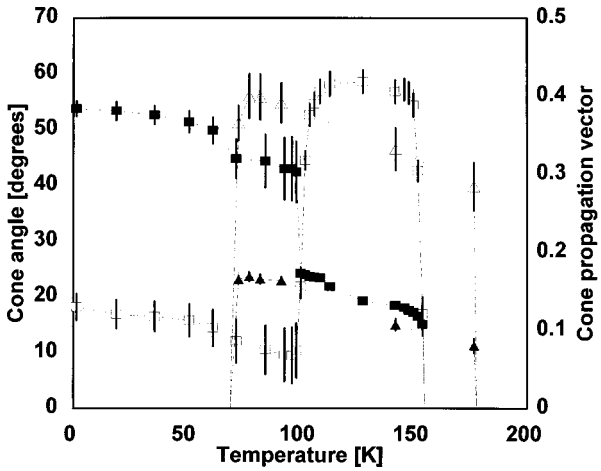

FIG. 7. Changes in the cone angle (open symbols) and propagation vector (filled symbols) of the cone as a function of temperature at zero pressure (squares) and with the cell clamped at 5 kbar at room temperature (triangles). The lines are guides to the eye.

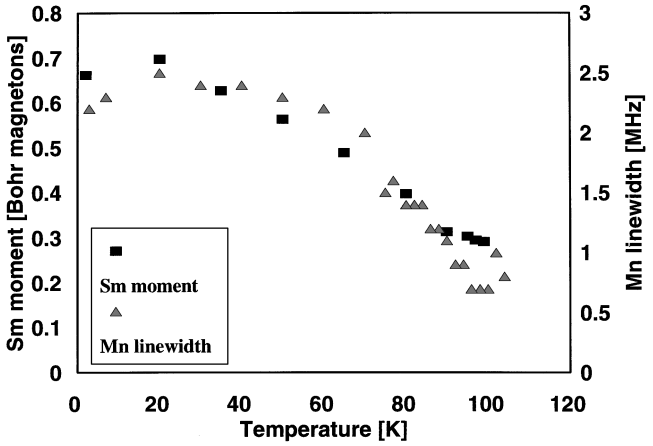

FIG. 8. Temperature variation of the Sm moment, and the Mn linewidth. Changes in both the Sm moment and cone angle (open squares in Fig. 7) may contribute to changes in the Mn linewidth.

Below around 70 K the structure is similar to the low-temperature phase FM2c [Fig. 3(a)] obtained at ambient pressure. The magnetic structure under 5 kbar, however, is commensurate with the nuclear structure (i.e., there is no cone). We therefore call this structure FM2. The total Mn moment is about $3.2\mu_B$. The confidence limits on the refinement with the sample in the pressure cell are about $0.15\mu_B$.

From about 73 to 230 K the structure is identical to that observed between 100 and 154 K at ambient pressure [Fig. 3(b)]. Changes in the propagation vector are shown in Fig. 7 (filled triangles). Above 177 K the ordering is commensurate. The open triangles in Fig. 7 show changes in the cone angle. The total moment amounts to $2.6\mu_B$.

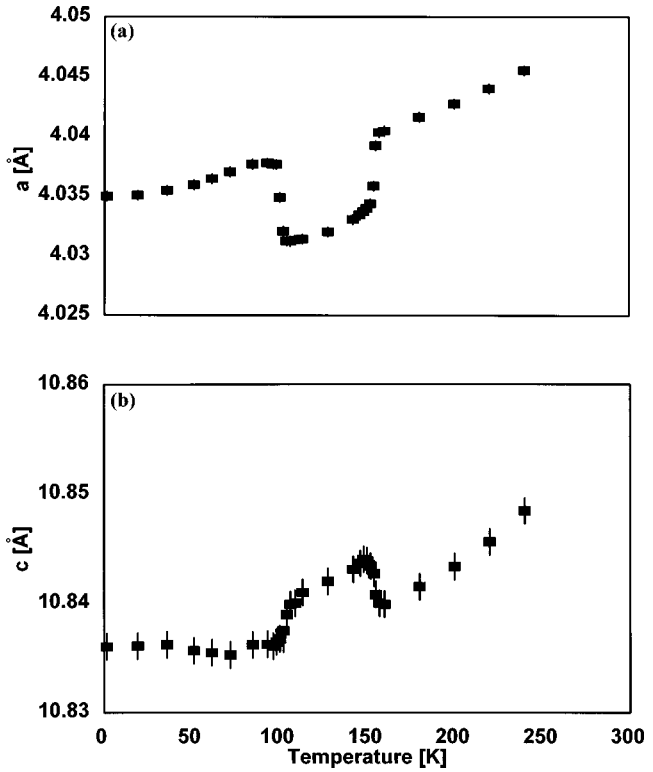

FIG. 9. Thermal variation of the lattice constants (a) in the *a* direction and (b) in the *c* direction.

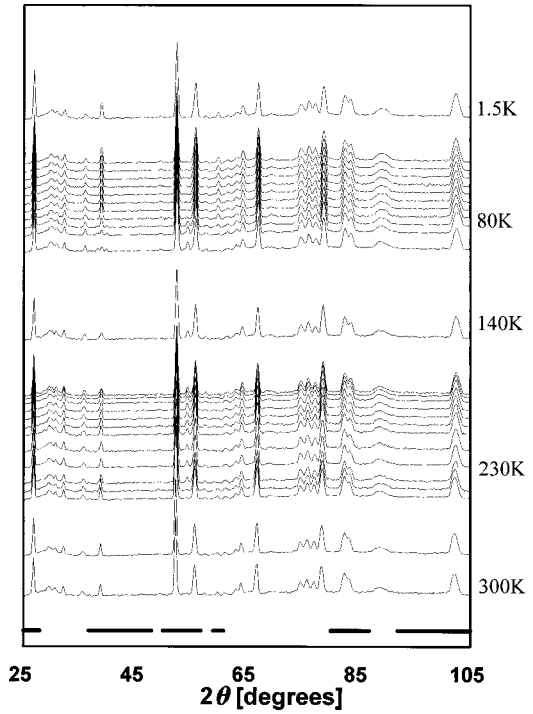

FIG. 10. Neutron thermogram of $SmMn_2Ge_2$ with 5 kbar clamped in at room temperature. Temperatures are indicated for some spectra. The regions excluded from the refinement due to background contributions from the cryostat and pressure bomb are indicated by the gaps in the bold line at the base of the thermogram.

Above ~230 K, measurements were made at around 237 and 276 K. The magnetic structure is similar to that at ambient pressure above 154 K, with a FM component in the *c* direction and an *a*-*b* plane AFM component [Fig. 3(c)]. The Mn moment decreases from the $2.6\mu_B$ value as the paramagnetic regime is approached.

Changes in the lattice parameters *a* and *c* are shown in Figs. 11(a) and 11(b), respectively. The abrupt changes (seen most clearly for the *a* parameter) clearly reflect the transitions between the different magnetic structures.

The results of the neutron-scattering measurements for the sample clamped with 10 kbar in the cell at room temperature are shown in Fig. 12 and are detailed below. As expected, the preferred orientation is larger when the cell is clamped at 10 kbar than at 5 kbar.

The low-temperature FM phase (existing as the incommensurable phase FM2c below 100 K at ambient pressure, and as the commensurable phase FM2 below 70 K with the cell clamped at 5 kbar) is limited to temperatures below 44 K with the cell clamped at 10 kbar. As with the cell clamped at 5 kbar, the magnetic structure is the commensurable structure FM2. It exhibits a total Mn moment of $2.9\mu_B$, consisting of a $2.3\mu_B$ FM component in the *a*-*b* plane and a $1.7\mu_B$ AFM component in the *c* direction.

The region of stability of the intermediate net AFM phase [see Fig. 3(c)], at this high pressure, has increased to 50–280 K. The magnetic structure is the commensurable structure AFM1 across the whole region of stability. This is unlike the situation at ambient pressure, where the incommensurable AFM1c is stable, or the situation in the cell clamped at 5 kbar where AFM1c is stable below 177 K and AFM1 is

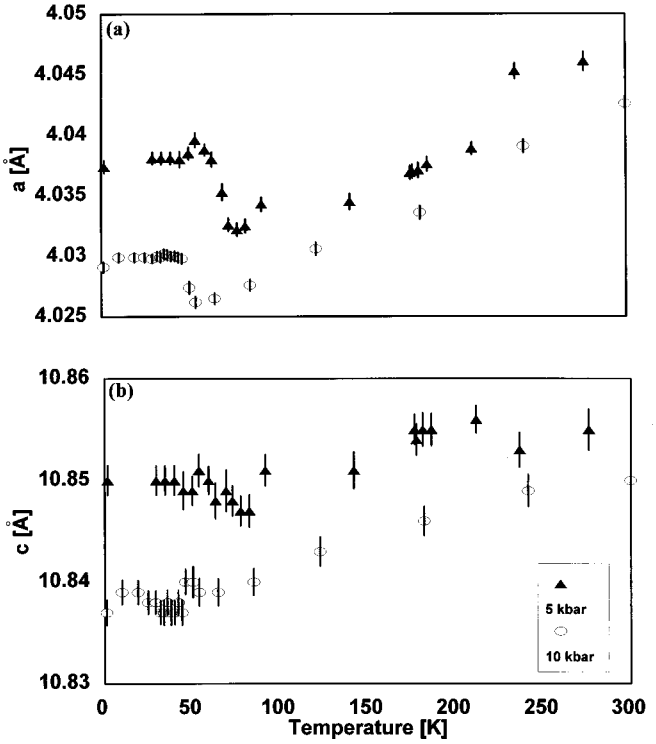

FIG. 11. Thermal variation of the lattice constants (a) in the *a* direction and (b) in the *c* direction, for the sample in cell with 5 and 10 kbar clamped at room temperature. The error bars are indicative of the reliability of the refinement to the data. The refinement under pressure includes an orientation parameter, not included in Fig. 9.

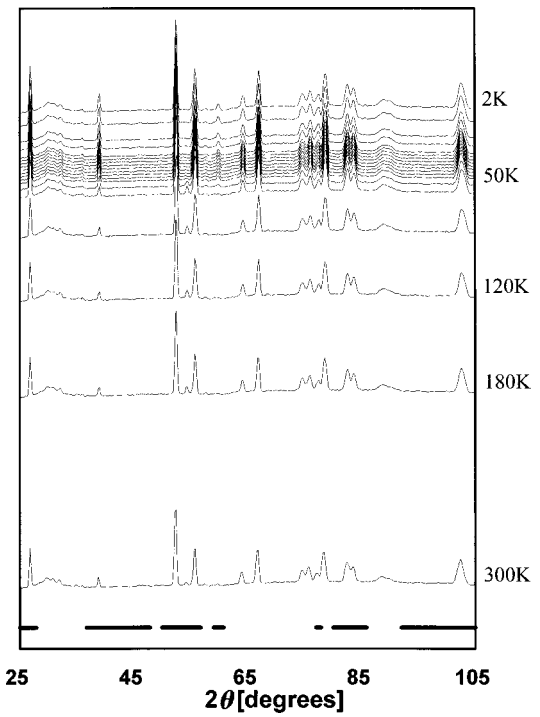

FIG. 12. Neutron thermogram of $SmMn_2Ge_2$ with 10 kbar clamped in at room temperature. Temperatures are indicated for some spectra. The regions excluded from the refinement due to background contributions from the cryostat and pressure bomb are indicated by the gaps in the bold line at the base of the thermogram.

stable above 177K. The total Mn moment in this temperature range is between $2.4\mu_B$ and $2.3\mu_B$.

At 300 K, the magnetic structure starts to show FM contributions, with a coupling similar to the one depicted in Fig. 3(c). The total Mn moment has, however, already decreased to below $2\mu_B$ as the system is close to becoming paramagnetic.

Figure 11 shows rapid changes in the lattice parameters due to thermal expansion near 50 K. These changes are associated with changes in the magnetic structure.

There is no evidence of a cone structure in any of the magnetic states when the cell is clamped at 10 kbar, and, as with our ac susceptibility and NMR measurements, there are no magnetic anomalies around 150 K under pressure. There is also no significant change in the thermal expansion at 150 K, as seen in Fig. 11.

IV. DISCUSSION

The data presented here provide evidence for the presence of a cone structure in $SmMn_2Ge_2$. The presence of incommensurate cone structures has been confirmed for a range of other systems with the $ThCr_2Si_2$ structure, particularly at low temperatures, and appears to arise as a result of the competition between intraplanar and interplanar Mn-Mn interactions. Cone structures have been observed in $LaMn_2Ge_2$,[12] $CeMn_2Ge_2$, $PrMn_2Ge_2$, and $NdMn_2Ge_2$.[13] Complex incommensurate structures have also been observed in $HoMn_2Ge_2$ (Ref. 14) and in $La_{1-x}Y_xMn_2Ge_2$ $(x<0.7)$.[15]

Neutron-scattering studies appear to indicate that compounds in the $R\ Mn_2X_2$ family with intraplanar Mn-Mn distances greater than about 2.85 Å(corresponding to lattice spacing of $a=4.031$ Å) have an AFM component between Mn neighbors in the (001) planes, whereas for Mn-Mn distances smaller than this, the ordering in the (001) planes is purely FM.[13] Figures 9 and 11 show that in the AFM1 state the lattice parameter in the *a* direction is closer to 4.031 Å than in the FM1 or FM2 states, and we find that it is the AFM1c state that has the smallest AFM component within the (001) planes ($1.6\mu_B$ compared with $2.2\mu_B$ for FM2 and $1.9\mu_B$ for FM1). The AFM1c state also exhibits the largest net FM component in the *c* direction within each (001) plane. Thus the anisotropic changes in the shape of the unit cell clearly reflect the importance of the intraplanar Mn-Mn interaction. These observed changes in the magnetic structure also provide an explanation of the anomalous GMR in the basal plane[5] in terms of a spin-valve mechanism. The application of a magnetic field along the *c* axis produces a metamagnetic transition from the AFM1c state to a FM state (presumably similar to FM1) with a larger AFM component in the (001) planes.

Figure 8 shows the low-temperature variation of the Sm moment in the refinement. The figure also shows a similar variation in the linewidth of the Mn NMR signal as a function of temperature. In the earlier paper by Lord *et al.*,[6] it was suggested that the changes in the linewidth were either indicative of changes in the Sm moment or were the result of changes in a noncollinear Mn magnetic structure. Our data indicate that there is a close correlation between the evolution of the Sm moment and changes in the magnetic structure of the Mn sublattice, including changes in the cone angle, as

shown by the open squares in Fig. 7. It seems likely that both these processes are affecting the linewidth of the Mn NMR resonance line. The changes in the ^{55}Mn frequency with temperature, shown in Fig. 5, may also be affected by both processes. The shape of the curve has $\partial^2\nu/\partial T^2$ largely negative in the regime in which changes of both the Sm moment and the cone angle could contribute to the change of slope, whereas $\partial^2\nu/\partial T^2$ is largely positive in the regime in which the cone has collapsed. It has been noted[6] that the ν versus P curves have a change of slope at 5 kbar in the FM2 state, and this may have been indicative of the disappearance of the cone structure in that sample. The low-temperature cone phase in the $^{154}SmMn_2Ge_2$ sample may therefore have collapsed at a pressure close to the low-temperature pressure in the 5 kbar clamped cell (i.e., around 3 kbar), but further measurements are required to confirm this.

Refinements of the neutron-scattering data indicate that a Sm moment may be present in the high-temperature FM regime, though the reliability of the refinement of the Sm moment decreases with increasing temperature. It therefore remains inconclusive whether the FM2-AFM1 ordering is driven by a collapse of the Sm moment. A reliable refinement of the Sm moment also proved to be difficult when the sample was in the pressure cell. This was in part due to the larger background from the pressure cell, but was also due to the close association between the Sm moment and the preferred orientation parameter in the refinement process. We were therefore unable to confirm earlier NMR findings,[6] which indicated that the magnetization of the Sm sublattice was unaffected by pressures of up to 6.1 kbar.

The anomaly at $T_{cc}=153$ K in the zero applied pressure ac susceptibility measurements, Fig. 4, appears to correspond to the temperature at which the collapse of the cone structure is observed. As shown in Fig. 7, the temperature at which the cone collapses is relatively independent of the applied pressure, compared with the changes in T_{t2}. This is consistent with the findings of Saha *et al.*[8] that T_{cc} is unaffected by the ''chemical pressure'' imposed by the partial substitution of Ge by Si. Furthermore, we observe no anomaly in the ac susceptibility in the high-pressure regime (8.8 kbar) where we observe no cone structure. It does appear, however, that the application of ''chemical pressure'' is not the same as the application of hydrostatic pressure. Saha and Ali[8] have observed the anomaly in $SmMn_2(Ge_{0.85}Si_{0.15})_2$ at a Si substitution corresponding to a hydrostatic pressure of 10 kbar, and our own preliminary neutron-scattering data on $SmMn_2(Ge_{0.9}Si_{0.1})_2$ powder show no evidence for the presence of a cone structure at any temperature.

A further phase transition below 30 K was indicated by the resistance data of Mallik, Sampathkumaran, and Paulose[16] and Sampathkumaran, Paulose, and Mallik,[17] though the authors could detect no anomaly in the heat capacity. We also could not detect this transition by NMR, ac susceptibility, and neutron scattering.

The T-P magnetic phase diagram of $SmMn_2Ge_2$, as proposed in Fig. 2, provides a summary of the results of the current study. Further measurements are required to identify the exact pressures above which the cone structures are no longer stable. The key to understanding the phase diagram lies in an understanding of the Mn-Mn and Mn-Sm interactions, and how they vary with interatomic spacing. One method of altering the effective interatomic spacing is by the partial substitution of the constituents. Further work is therefore in progress to investigate the magnetic properties and T-P phase diagram of the system $SmMn_2(Ge_{1-x}Si_x)_2$.

V. CONCLUSIONS

Neutron scattering, ac susceptibility, and NMR measurements were made on isotopically enriched $^{154}SmMn_2Ge_2$. This sample produced much clearer neutron-diffraction spectra than in a previous study using a sample containing natural abundance Sm. The structure of all the magnetic states was investigated. A temperature versus pressure magnetic phase diagram was proposed. The system behaved as a reentrant ferromagnet, but was more complicated than suggested in previous studies. The phase diagram consisted of six distinct magnetic states. At low temperatures and pressures, incommensurate cone structures were observed. The antiferromagnetic state was characterized by a $1.6\mu_B$ antiferromagnetic component of the Mn moments within the (001) planes, whereas in the magnetic states with a net ferromagnetic moment, antiferromagnetic components of the moments in the (001) planes were significantly larger ($2.2\mu_B$ and $1.9\mu_B$ for the low- and high-temperature ferromagnetic structures, respectively). This provided an explanation for the anisotropic change in the lattice constant and for the changes in magnetoresistance in $SmMn_2Ge_2$ systems. It was found that the Mn-Mn spacing dropped close to 2.85 Å in the antiferromagnetic state, the threshold spacing below which only ferromagnetic coupling in the (001) planes has been observed in a range of related systems.

ACKNOWLEDGMENTS

We gratefuly acknowedge the EPSRC for financial support and would like to thank Professor R. Cywinski for his interest and encouragement.

*Author to whom correspondence should be addressed: SMC, DERA, Farnborough, Hants, GU14 OLX, UK.

[1] A. Szytula and J. Leciewicz, in *Handbook on the Physics and Chemistry of the Rare Earths*, edited by K. A. Geschneidner, Jr. and L. Eyring (Elsevier, Amsterdam, 1989), Vol. 12, p. 133.

[2] H. Fujii, T. Okamoto, T. Shigeoka, and N. Iwata, Solid State Commun. **53**, 715 (1985).

[3] E. M. Gyorgy, B. Batlogg, J. P. Remeika, R. B. van Dover, R. M. Fleming, H. E. Bair, G. P. Espinosa, A. S. Cooper, and R. G. Maines, J. Appl. Phys. **61**, 4237 (1987).

[4] G. J. Tomka, Cz. Kapusta, C. Ritter, P. C. Riedi, R. Cywinski, and K. H. J. Buschow, Physica B **230**, 727 (1997).

[5] R. B. van Dover, E. M. Gyorgy, R. J. Cava, J. J. Krajewski, R. J. Felder, and W. F. Peck, Phys. Rev. B **47**, 6134 (1993).

[6] J. S. Lord, P. C. Riedi, G. J. Tomka, Cz. Kapusta, and K. H. J. Buschow, Phys. Rev. B **53**, 283 (1996).

[7] J. S. Lord, P. C. Riedi, Cz. Kapusta, and K. H. J. Buschow, Physica B **206&207**, 383 (1995).

[8] S. Saha and N. Ali, J. Appl. Phys. **79**, 5233 (1996).

[9] Y.- Wang, F. M. Yang, N. Tang, J. F. Hu, K. W. Zhou, C. P.

Chen, Q. D. Wang, and F. R. Boer, J. Appl. Phys. **80**, 6898 (1996).
[10] G. J. Tomka, Cz. Kapusta, C. Ritter, and P. C. Riedi, J. Magn. Magn. Mater. **177**, 821 (1998).
[11] J. S. Lord and P. C. Riedi, Meas. Sci. Technol. **6**, 149 (1995).
[12] G. Venturini, R. Welter, E. Ressouche, and B. Malman, J. Alloys Compd. **210**, 209 (1994).
[13] R. Welter, G. Venturini, E. Ressouche, and B. Malman, J. Alloys Compd. **218**, 204 (1995).
[14] G. Venturini, B. Malman, and E. Ressouche, J. Alloys Compd. **240**, 139 (1996).
[15] G. Venturini, B. Malman, and E. Ressouche, J. Alloys Compd. **241**, 135 (1996).
[16] R. Mallik, E. V. Sampathkumaran, and P. L. Paulose, Physica B **230**, 731 (1997).
[17] E. V. Sampathkumaran, P. L. Paulose, and R. Mallik, Phys. Rev. B **54**, R3710 (1996).